

# THE EFFECT OF ADDING SMALL AMOUNTS OF ZNO IN COMPACTED BOVINE HYDROXYAPATITE FOR BIOMEDICAL APPLICATIONS

Muhammad Waziz Wildan dan Muhammad Kusumawan Herliansyah

Department of Mechanical Engineering & Industrial Engineering  
Faculty of Engineering, Gadjah Mada University  
Jl. Grafika 2 (55281)  
Yogyakarta, Indonesia

Phone: +62-274-521673, FAX: +62-274-521673, E-mail: m\_wildan@ugm.ac.id

## ABSTRACT

*This work is concerned with the effect of trace element amount (%wt) in the properties of the sintered bovine hydroxyapatite (BHA). The BHA powders were mixed with various percentage of ZnO ranging from 0 wt. % to 15 wt. % by magnetic stirrer. The dry powders were uniaxially pressed at 312 MPa. For comparison purpose, synthetic HA also produced using the same process. It has been found that the relative density decreases with increasing of ZnO content.*

*The additions of ZnO have shown an increasing of Vickers hardness with the highest of the micro Vickers hardness obtained in 1.5 wt. % ZnO. The BHA have stable phase stability at within the range of 0.5 wt% to 1.0 wt% and 2.0 wt% to 5.0 wt. %. The decomposition occurs as the ZnO increased to 10 wt. % and 15 wt. %. Thus, material preparation plays an important role on determining the effect of sintered BHA.*

*Keyword:* Bovine Hydroxyapatite, trace elements, ZnO, Vickers hardness.

## 1. Introduction

Bone graft is an operative treatment that repairs the bone defects due to traumatic or non traumatic events. Generally, the common indications for bone grafting are bone loss, requiring mechanical support and structural replacement [1]. Moreover, bone grafting is intended to stimulate bone healing and fill the bone defects. The supply for natural bone grafting is limited. Although autologous bone grafting is the standard gold treatment to repair a bone defects, it also posses some problems such as post operation pain, blood loss, low mechanical strength and available in limited supply [1].

Allograft could be used as an alternative but the main risk is the possibility transmission of infections (e.g HIV, Hepatitis, etc) and may be rejected by the human body [2,3]. For this reason, there is a growing need for fabrication of artificial hard tissue replacement implants. In addition, xenograft could be used as an alternative for bone defects. Xenograft, usually bovine origin is easy to obtain at lower cost and available in unlimited supply. The inorganic component which is hydroxyapatite (HA) is similar to human bone. This makes xenograft are biocompatible, and are slowly resorbed and replaced by bone [4].

Currently, hydroxyapatite become the material of choice for dental and medical surgery.. Among the most important properties of HA is its excellent

biocompatibility and form a direct chemical bond with hard tissues [5]. HA derived from bovine bone has great potential as bone substitute due to is biocompatibility and osteoconductive properties. Synthetic HA, however have low mechanical properties especially when exposed in wet environment [6].

Dense HA widely used as percutaneous devices for continuous ambulatory peritoneal dialysis, monitoring of blood pressure and blood sugar, or optical observation of inner body tissue [7]. Bone also reported to adhere strongly to dense HA implants [8]. In dental surgery, dense HA has been used as artificial tooth roots. However, the use only limited to unloaded tooth root substitutes due to poor mechanical properties [3]. Thus, there is a necessity to develop a dense bone graft with superior mechanical properties and biocompatibility since dental enamel in tooth especially in adult body unable to regenerate itself.

Zn as a trace element become a choice because it's presence in all biological tissues and its diverse role in biological functions [9]. Zn has been reported to be involved in bone metabolism and stimulates bone formation in human and many animals [10]. In addition, Zn may also be involved in the process of wound healing [11].

In this study, a new composite of bovine hydroxyapatite (HA) reinforced with ZnO is developed.



Beside that, the effect of ZnO as a trace element is characterized in the properties of sintered HA.

## 2. Experimental Procedure

### 2.1 Material Preparation

HA, derived from bovine bone (BHA) was ground using mortar and pestle to get smaller particle size. After that, the powders were sieved using sieve shaker machine (Retsch AS200) to get small particle distribution. Almost 50% of the particle size used in this research is between 150 $\mu$ m and 300 $\mu$ m. The BHA powder mixed with ten different percentage of ZnO which are 0, 0.5, 1.0, 1.5, 2.0, 2.5, 3, 5, 10, and 15 wt.% using distilled water as a solution agent. For comparison, synthetic commercial HA (Sigma Aldrich: 04238) also doped with same amount of ZnO. The solution was mixed by mortar and pestle for 10-15 minutes before mixed by magnetic hot plate stirrer for 60 minutes. The wet solution was put inside incubator to get dry powder.

### 2.2 Sample Preparation

Each powder from each sample was weighed using Precisa (XT220A, Switzerland). The weighed powder were uniaxially pressed at 312 MPa to cylindrical pellets with diameter of 20 mm. The green compacts of HA were sintered until 1200°C to provide strength to a finished material.

### 2.3 Characterization

The density of the sintered samples was calculated from the dimensions measured with vernier caliper and weight measured by analytical balance. The relative density obtained by taking theoretical density both of types of HA as 3.156 g.cm<sup>-3</sup> while relative porosity obtained by subtracting relative density with 100. Microhardness test were done with a Vickers microhardness testing unit (load 245.2 mN). The microstructure of sintered HA was observed by scanning electron microscopy (Philips XL40) at magnification between 1000x and 8000x using acceleration voltage of 20 kV. The phases of the samples were identified by using X-ray diffraction analysis (XRD, Siemens D5000) with monochromatic radiation of Cu K $\alpha$ . The operation took place at 40kV and 30mA with having the surface radiation level at 0.5 mSv per hour. Spectra were recorded from 2 $\theta$  equals to 10.01° to 79.99° with step scan of 0.02°. The identification of phases performed were compared with the standards complied by the Joint Committee on Powder Diffraction Standards (JCPDS data file No. 9-432). The chemical features of sintered BHA and HA were identified by using Fourier Transform Infra-Red spectroscopy (FTIR, Perkin Elmer Instruments, Spectrum RX1) equipped with DTGS-KBr window detector using KBr pellets at a ratio of 1 mg sample per 300 mg KBr (Figure 3.13). The transmission

IR spectra were recorded over the range of 370–4000 cm<sup>-1</sup> with 1 cm<sup>-1</sup> resolution averaging 100 scans.

The HA was milled together with the potassium bromide (KBr) to form a very fine powder. This powder is then compressed into a thin pellet which it can be analyzed. KBr is being used because due to its transparency in the IR wavelength region.

## 3. Results and Discussions

### 3.1 General Observation

A direct observation made after the sintering process shows that the colors change of the samples. Before sintering, all the samples BHA and synthetic HA are white in color. After sintering in box furnace up to 1200°C, the synthetic HA samples became blue while BHA samples remained white.

Generally, the color of the mineral is related to some impurities or defects. Furthermore, the crystal structure of HA powder also determines the color change [12]. Synthetic HA material has hexagonal space group P63/m with a molecule of Ca10(PO4)6(OH)2 in the unit cell. In the other hand, BHA is a natural material obtained from bovine bone which contains small percentage of other elements such as carbonate, magnesium and sodium. In bone, natural HA is present in the form of microcrystalline platelets. In view of this, crystal structure is the decisive factor of the color change.

The blue color appears at the synthetic HA samples are believed due to the existence of manganese content. Previous research also confirmed that synthetic HA containing manganese shows a blue color after sintering at high temperature in an oxidizing atmosphere [12]. Otherwise, BHA samples remain white because the inorganic component, which is HA only, contains small percentage of trace elements such as carbonate, magnesium, and sodium. This means that other impurities cannot affect the color change except manganese.

### 3.2 Relative Density

The effect of ZnO addition on the relative density and linear shrinkage of synthetic HA and BHA are shown in Fig. 1 and Fig. 2. The percentage of linear shrinkage of HA was higher than that of BHA. Maximum linear shrinkage of HA is 18.58% occurs at 5% of ZnO while maximum linear shrinkage of BHA is 8.92% occurs at 10% of ZnO. Linear shrinkage of sintered HA were higher than that of BHA due to the particle size distribution. Particle sizes of HA 04238 were smaller than BHA, so they have higher surface area and contact area.

It was found that the relative density of the BHA and HA-04238 is in decreasing trend as percentage of ZnO increased. The maximum relative density in BHA is 81.644 g/cm<sup>3</sup> (for specimen with 1.5% ZnO). Otherwise, the maximum relative density of HA-04238 is



96.457 g/cm<sup>3</sup> (for specimen with 0% ZnO). Usually, a possible reason in reducing density is due to the decomposition of HA into another calcium phosphate [13]. However, the decrease in density also would be due to loss of water by dehydroxylation of HA during sintering process [14]. These can be confirmed by the following methods which are XRD, FTIR and SEM.

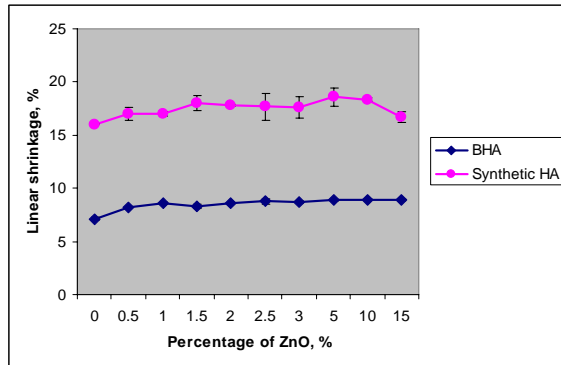


Fig 1. Linear shrinkage of BHA and synthetic HA

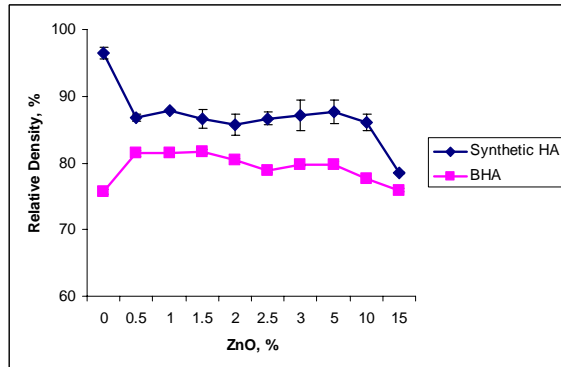


Fig 2. Relative density of BHA and synthetic HA

According to Fig 2, the relative porosity obtained is increasing as the percentage of ZnO increased. The porosity is related to the pores formed in the sample. The pores formed because of irregular powder sizes and by controlling sintering rate, the pores can be removed.

### 3.3 Vicker Hardness

Fig. 3 presents the microhardness of BHA and synthetic HA-04238. A maximum hardness of BHA was found at 1.5% of ZnO while synthetic HA was found at 2.5% of ZnO. The microhardness of the samples start decreasing after achieved the maximum value. The decreasing rate occurs as the ZnO increasing. This is because the presence of high percentage of ZnO will make the samples vulnerable to high temperature and may lead to abnormal grain growth, decompose into other calcium phosphate and produce large pores which affect the mechanical properties [3, 15]. In the other

hand, there are possibilities for the indenter pressed at the area where the distributions of ZnO are higher than other area in a sample or pressed at the area where the porosity is high. The decrease of hardness also can be related to the porosity of the sample. When the porosity is increasing the grain size is also increasing and results of poor hardness. By comparing between two of them, the microhardness of BHA is smaller than synthetic HA is due to its particle size.

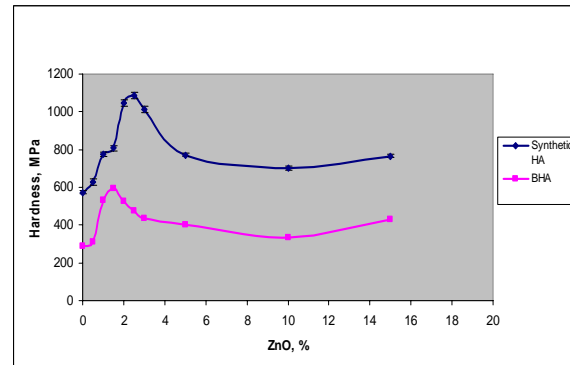


Fig 3. Microhardness of BHA and synthetic HA

### 3.4 Microstructure Analysis

The results of SEM images of BHA and synthetic HA are shown in the Fig 4. The images shows that the particles were adhere to each other after sintering process. The pore size observed was varied, but roughly less than 10  $\mu$ m. The formation of closed pores also detected in the samples. The closed pores establish due to non-uniform powder compaction during sample preparation with irregular powder sizes and wide particle distribution. The closed pores reported will limit the final density of the sample and may lead to decreasing of mechanical properties as discussed by previous research [13]. The comparison made between BHA and synthetic HA shows that the pore formation in synthetic HA is less due to small particle size which result high hardness as discussed before.



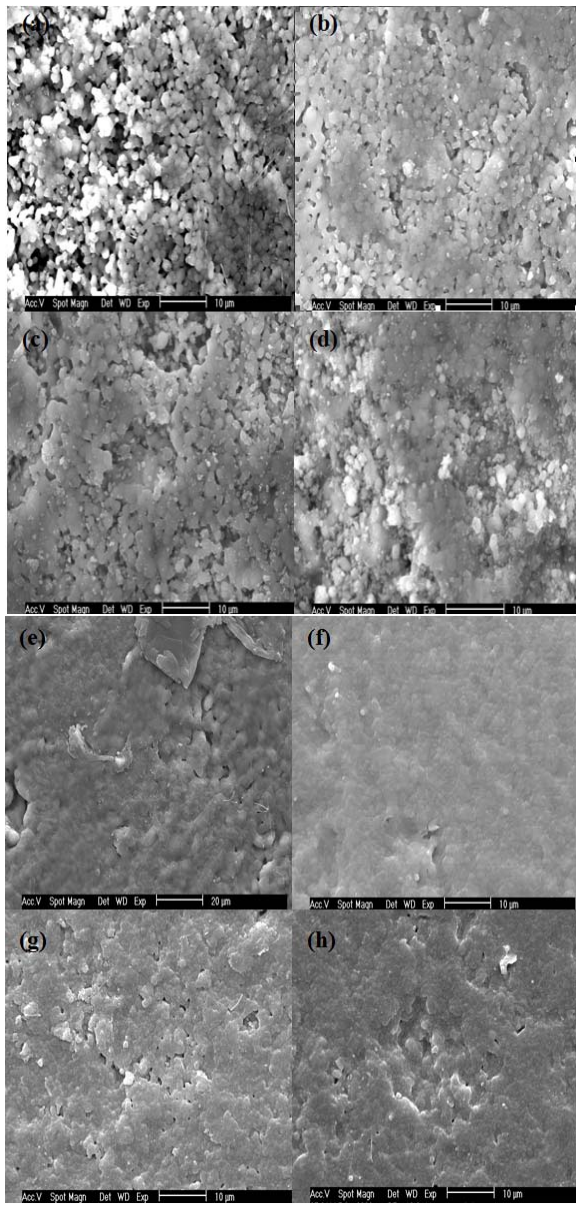


Fig 4. SEM images (a) 0.5 wt% ZnO+BHA, (b) 1.5 wt% ZnO+BHA, (c) 5.0 wt% ZnO+BHA; (d) 10.0 wt% ZnO+BHA, (e) 0.5 wt% ZnO+HA , (f) 1.5 wt% ZnO+HA, (g) 5.0 wt% ZnO+HA, (h) 10.0 wt% ZnO+HA

### 3.5 XRD Phase Analysis

The XRD pattern of BHA and synthetic HA are shown in the Fig 5 and Fig. 6. The XRD pattern shows that the samples were in crystalline structure. The most prominent peak observed was in the range of  $30^\circ$  to  $35^\circ$  2-theta degree. All the samples in BHA show consistent pattern except 1.5 wt% ZnO, 10 wt% ZnO, and 15 wt% ZnO. By referring to the standard JPDSCards data file, the decomposition into  $\beta$ -TCP took place in the 1.5 wt%

ZnO at 20 angles of  $27.75^\circ$  and  $31.01^\circ$ . In addition, the partial decomposition of BHA into TTCP observed at  $36.19^\circ$  and  $36.25^\circ$  of 10 wt% ZnO and 15 wt% ZnO. By comparing to synthetic HA, the decomposition into  $\alpha$ -TCP took place at 1.0 wt% at 20 angles of  $30.79$  and  $31.43$  while TTCP appear only at 10 wt% ZnO. The present XRD results suggest that the BHA has good phase stability in the range of 2.0 wt% ZnO to 5.0 wt% ZnO. However, the presence of TCP affects the mechanical strength and material will have high biodegradability [3].

Although the decomposition was not detected in other samples, it should be noted that the dehydroxylation could have taken place. This can be observed by comparing the XRD peaks positions of the prominent peaks with the standard JPDSCards data for stoichiometric HA [14]. Table 1 and 2 present the position of three most prominent peaks obtained in XRD pattern that corresponds to the plane (211), (112), and (300). The results show that dehydroxylation has occurred at the sample during sintering process.

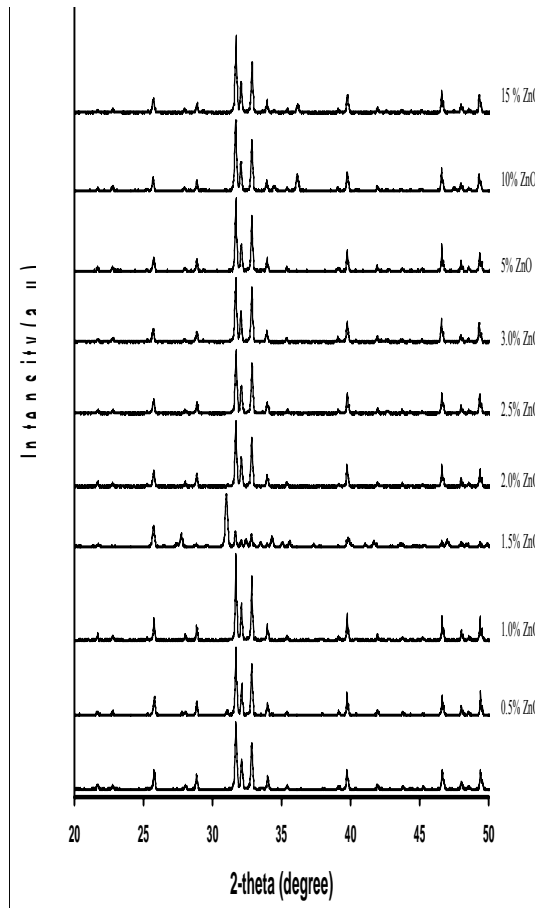


Fig. 5. XRD peaks of BHA



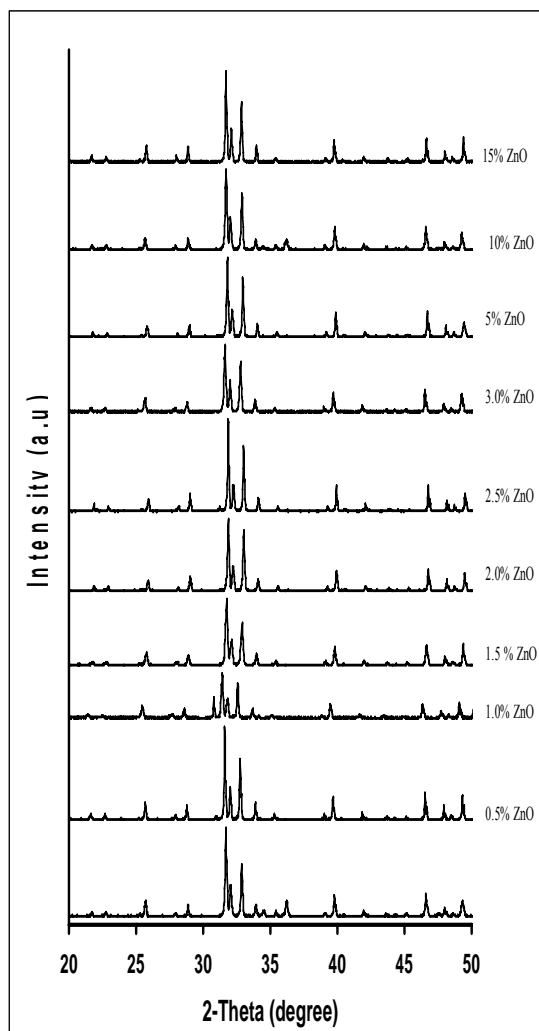


Fig. 6. XRD peaks of synthetic HA

Table 1. Positions of XRD peaks of BHA

|                    | 20( $^{\circ}$ ) at variation percentage of ZnO |                    |                    |
|--------------------|---|--------------------|--------------------|
|                    | (211) <sup>a</sup>                              | (112) <sup>a</sup> | (300) <sup>a</sup> |
| Standard           | 31.773  | 32.196             | 32.902             |
| 0.5 wt.%           | 31.710  | 32.130             | 32.850             |
| 2.5 wt.%           | 31.730  | 32.090             | 32.870             |
| 3.0 wt.%           | 31.710  | 32.070             | 32.850             |
| 10.0 wt.%          | 31.690  | 32.050             | 32.850             |
| 15.0 wt.%          | 31.710  | 32.070             | 32.870             |
| Maximum difference | 0.083   | 0.146              | 0.052              |
| Minimum difference | 0.043   | 0.066              | 0.032              |

<sup>a</sup> (hkl)

Table 2. Positions of XRD peaks of synthetic HA  
20 ( $^{\circ}$ ) at variation percentage of ZnO

|                    | (211) <sup>a</sup> | (112) <sup>a</sup> | (300) <sup>a</sup> |
|--------------------|--------------------|--------------------|--------------------|
| Standard           | 31.773             | 32.196             | 32.902             |
| 0.5 wt.%           | 31.610             | 32.030             | 32.770             |
| 2.5 wt.%           | 31.850             | 32.270             | 33.010             |
| 3.0 wt.%           | 31.650             | 32.010             | 32.790             |
| 15.0 wt.%          | 31.710             | 32.110             | 32.850             |
| Maximum difference | 0.163              | 0.186              | 0.132              |
| Minimum difference | 0.077              | 0.074              | 0.108              |

<sup>a</sup> (hkl)

### 3.6 FTIR Analysis

The FTIR spectrum of BHA and synthetic HA at various percentages of ZnO are shown in Fig. 7 and Fig. 8. FTIR was done to investigate the main groups in HA compound. There are three main groups present in FTIR spectrum which are hydroxyl ( $\text{OH}^-$ ), carbonate ( $\text{CO}_3^{2-}$ ), and phosphate ( $\text{PO}_4^{3-}$ ). Generally, the FTIR spectra of all samples matched with spectra of pure HA (0 wt.% ZnO) and in agreement with literature data on HA [6,16]. In BHA samples, hydroxyl group can be observed at  $3449 \text{ cm}^{-1}$  and  $571 \text{ cm}^{-1}$ . However, the pronounce peak of hydroxyl only can be obtain at  $572 \text{ cm}^{-1}$ . As the percentage of ZnO increased, the intensity of  $\text{OH}^-$  at band  $3404 \text{ cm}^{-1}$  decreased and almost cannot be seen. The same thing also happens in synthetic HA-04238. The hydroxyl group at band  $3404 \text{ cm}^{-1}$  has less intensity compared with hydroxyl group at band  $572 \text{ cm}^{-1}$ . This result is related with the XRD analysis which shows that dehydroxylation occurs on the samples.

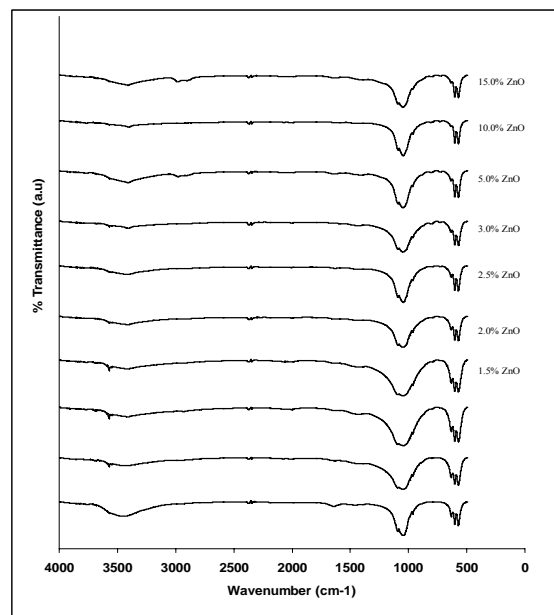


Fig. 7. FTIR peaks of BHA



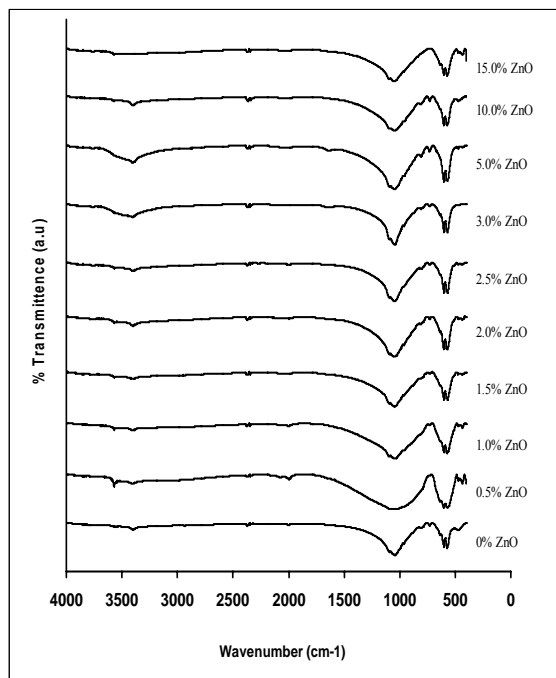


Fig. 8. FTIR peaks of synthetic HA

#### 4. Conclusion

1. Additions of ZnO have shown mechanical changes on properties of sintered HA. The highest Vickers hardness is found on specimens in the range of 1.5 wt.% to 2.5 wt.% ZnO.
2. The presence of  $\alpha$ -TCP,  $\beta$ -TCP, and TTCP should be avoided because it will increase the biodegradability of HA ceramics.
3. Dehydroxylation took place at the sample, as evidenced by decreasing in densification.
4. The closed pores formed on the sample affect the mechanical properties of the sintered HA. Material and sample preparation is a crucial stage because good microstructures morphology strongly depends on the powder packing and powder properties.

#### Acknowledgements

This work was supported by a grant (DPP/SPP) from the Faculty of Engineering Gadjah Mada University, Indonesia

#### References

- [1]. Doron, I., Ilan, M.D. and Army L.Ladd, MD (2003), "Bone Graft Substitutes", Operative Techniques in Plastic and Reconstructive Surgery.
- [2]. Grauer, JN, Beiber, JM, Kwon, B, Vaccaro, AR (2005), "The evolution of allograft bone for spinal applications", Orthopedics, Vol 28, pp. 573.
- [3]. Suchanek, W and Yoshimura, M. (1998), "Processing and properties of hydroxyapatite-based biomaterials for use as hard tissue replacement implant" J. Mat. Res., Vol.13, No. 1.
- [4]. Smiler, DG (1996), "Bone grafting: materials and modes of action, Pract Periodont Aesthetic Dent, Vol 8, pp. 413-416.
- [5]. Vallet-Regi M and Gonzalez-Calbet JM. (2004), "Calcium phosphate as substitution of bone tissues", Progress in Solid State Chem.stry, Vol 32, pp. 1-31.
- [6]. Ooi CY, Hamdi M, and Ramesh S. (2007), "Properties of hydroxyapatite produced by annealing of bovine bone", Ceramics international, Vol 33, pp. 1171-1177.
- [7]. Hench, L.L. (1991), "Bioceramics: From concept to clinic", J. Am. Ceram. Soc., Vol 74, No. 7, pp. 1487-510.
- [8]. Jarcho M, Jasty V, Gumaer KI, Kay JF and Doremus RH. (1978)."Electron microscopic study of a bone-hydroxyapatite implant interface. Biomed. Mater. Res. Symp Trans. 2, 112-113.
- [9]. Tang Y, Chappell HF, Dove MT, Reeder RJ, Lee YJ. (2009), "Zinc incorporation into hydroxylapatite", Biomat., Vol 30, pp. 2864-2872
- [10]. Ishikawa K, Miyamoto Y, Yuasa T, Ito A, Nagayama M, and Suzuki K. (2002), "Fabrication of Zn containing apatite cement and its evaluation using human osteoblastic cells", Biomaterials, Vol 23, pp. 423-428.
- [11]. Pories WJ and Strain WH, (1970), Zinc and wound healing. In: Zinc metabolism, AS Prasad, Ed., pp 378-394. Charles C Thomas, Springfield, IL.
- [12]. Yubao L, Klein CPAT, Xingdong Z, and Groot KD. (1993), "Relationship between the colour change of hydroxyapatite and the trace element manganese", Biomaterials, Vol 14, No. 13
- [13]. Thangamani N, Chinnakali K, Gnanam FD. (2002), "The effect of powder processing on densification, microstructure and mechanical properties of hydroxyapatite", Ceramic Int., Vol 28, pp. 355-362
- [14]. Wang PE and Chaki TK. (1993), "Sintering behaviour and mechanical properties of hydroxyapatite and dicalcium phosphate", J. of Mat. Sci. ; Mat. in Medicine, Vol 4, pp. 150-158
- [15]. Joon, B.P and Joseph, D.B. (2002), Biomaterials Principles and Applications, 2<sup>nd</sup> Edition, CRC Press, pp. 21-42.
- [16]. Joscheck S, Nies B, Krotz R, Gopferich A. (2000), "Chemical and physicochemical charazterization of porous ceramics made of natural bone", Biomaterials, Vol 21, pp. 1645-1658

